available at www.sciencedirect.com

ScienceDirect

journal homepage: www.elsevier.com/locate/ecolmodel

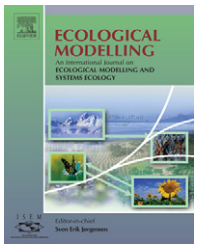

Modeling soil salinity distribution along topographic gradients in tidal salt marshes in Atlantic and Gulf coastal regions

Hongqing Wang[a,*], *Y. Ping Hsieh*[b], *Mark A. Harwell*[a,1], *Wenrui Huang*[c]

[a] *Environmental Cooperative Science Center, Environmental Sciences Institute, Florida A&M University, Tallahassee, FL 32307, USA*
[b] *College of Engineering Sciences, Technology & Agriculture, Florida A&M University, Tallahassee, FL 32307, USA*
[c] *Civil Engineering Department, College of Engineering, Florida A&M University and Florida State University, Tallahassee, FL 32310, USA*

ARTICLE INFO

Article history:
Received 16 March 2006
Received in revised form
31 August 2006
Accepted 16 October 2006
Published on line 22 November 2006

Keywords:
Soil salinity
Tidal inundation
Salt marsh
Elevational gradient
Simulation model
Atlantic and Gulf coasts

ABSTRACT

Soil salinity plays a very important role in determining the distribution of vegetation, plant productivity, and biogeochemical processes in coastal marsh ecosystems. Salinity gradients and salinity–vegetation associations in salt marshes have often been observed but rarely explained. A quantitative and systematic study on the soil salinity distribution in salt marshes is not only important to the understanding of coastal marsh ecosystems but also to the development of a potentially useful ecological and environmental indicator. In this research, we developed a salt marsh soil salinity model based on an existing salt and water balance model with modifications to several key features to examine the impacts of tidal forcing, climate, soil, vegetation, and topography on soil salinity distributions of the Atlantic and Gulf coastal marshes. This model was calibrated and validated using field observations from the St. Marks National Wildlife Refuge (NWR) of northwestern Florida, USA. The results showed that the model had good agreement ($r^2 = 0.84$, $n = 15$, $P < 0.001$) with field observations. We found that the mean higher high water (MHHW) level determines the location of the salinity maximum in a coastal salt marsh. Simulations indicate that tidal irregularity primarily controls the width of the salinity maximum band. Evapotranspiration, temperature, hydraulic conductivity, and incoming tidal salinity significantly affect the salinity maximum band, which may lead to the formation of salt barrens/flats when reaching a threshold level.
© 2006 Elsevier B.V. All rights reserved.

1. Introduction

Soil salinity, together with other soil physical and chemical properties, plays an important role in plant composition, productivity, and distribution (zonation) in coastal marsh ecosystems because of the differences in tolerances of plant species to salinity and tidal inundation (Adams, 1963; Mahall and Park, 1976a,b; Adam, 1990; Callaway et al., 1990; Pennings and Bertness, 1999; Hughes et al., 1998; Hsieh, 2004; Silvestri and Marani, 2004; Pennings et al., 2005). Therefore, the spatial and temporal variation in soil salinity is a critical part of salt marsh ecology. Tidal salt marshes typically consist of high, middle, and low marsh zones. Elevation of tidal marshes plays an important role in the structure and function of salt marsh ecosystems because it is directly related to inundation frequency and duration of tides (e.g., Adam, 1990; Silvestri and

* *Corresponding author at*: 1520 S. Bronough St. Science Research Center 305 D, Environmental Sciences Institute, Florida A&M University, Tallahassee, FL 32307, USA. Tel.: +1 850 412 5119; fax: +1 850 561 2248.
E-mail address: hong.wang@famu.edu (H. Wang).
[1] Current address: Harwell Gentile & Associates, LC, Palm Coast, FL 32164, USA.
0304-3800/$ – see front matter © 2006 Elsevier B.V. All rights reserved.
doi:10.1016/j.ecolmodel.2006.10.013

Marani, 2004). Previous field studies (e.g., Adams, 1963; Adam, 1990; Pennings and Callaway, 1992; Morris, 1995; Pennings and Bertness, 1999; Bertness and Pennings, 2000; Hsieh, 2004) have found that there is a soil salinity maximum band near the high marsh zone. One of the main reasons for the salinity increase above the mean high water (MHW) level is the decreased duration of the tidal inundation, which allows evapotranspiration to concentrate porewater salinity and salt to accumulate (e.g., Adam, 1990; Hsieh, 2004; Silvestri et al., 2005). This salinity gradient, therefore, is characteristic of a coastal marsh with respect to the interactions of tide, topography, climate, and vegetation factors (Mahall and Park, 1976a,b; Morris, 1995; Hsieh, 2004; Silvestri et al., 2005).

There are few quantitative and systematic studies on the effects of various factors, such as tide, climate, soil, topography, and vegetation, on the soil salinity gradient in a coastal marsh. Several questions need to be answered: (1) Is this soil salinity gradient a general feature of coastal marshes over a large geographic area? (2) If so, what are the main biophysical factors that affect the distribution and magnitude of the gradient? For example, we know that salt barrens/flats/pannes are commonly found in southern but not northern salt marshes (e.g., Pennings and Bertness, 1999). Apparently, this is driven by warmer climate of the south that enhances ET in general, but we cannot predict where the divide would be geographically. Limited field studies constrain our understanding of the relationship between soil salinity and environmental factors. As we know from previous studies and our own observation, only certain coastal areas will have the potential to develop salt barren/flats in a salt marsh, but we do not know exactly where (cf., Pennings and Bertness, 1999; Bertness and Pennings, 2000; Hsieh, 2004).

The objectives of this research are to use an ecosystem modeling approach to: (a) develop and calibrate a simulation model for predicting salinity distribution in the marsh; (b) examine the soil salinity distribution along a topographic gradient in a Gulf Coastal salt marsh; (c) examine the effects of major forcing (tide regime, climate, soil properties, and vegetation) on soil salinity in salt marshes along the Atlantic and Gulf coasts of the US.

2. Methods

2.1. *Model structure*

The salinity model was developed based on a previous model by Morris (1995). In Morris' model, water movement is assumed to be predominantly vertical with no groundwater input or lateral water flow. The concentration of salt is assumed to be uniformly distributed throughout a pedon of 1 m^2 and 30 cm deep. In the model, the hydrological processes include gravity drainage, infiltration, and ET. The processes that determine salt content are salt movements by drainage, infiltration, diffusion between the sediment and surface water, and vegetation secretion. Salt input via precipitation is assumed to be negligible.

In the model, the processes of water and salt transport vary with the site being flooded or exposed by comparing tide level with site elevation. If the site is flooded (tide height > site elevation), pore volume is filled with flooding seawater and reaches saturation. The salt content is determined by the balance between infiltration of salt from seawater and loss by diffusion between sediment and surface water. If the site is exposed (tide height < site elevation), pore water volume is determined by the balance among rainfall, ET, and drainage. Salt is lost by drainage and plant salt secretion driven by ET (Fig. 1). For details of these processes and the salt and water balance equations, refer to Morris (1995).

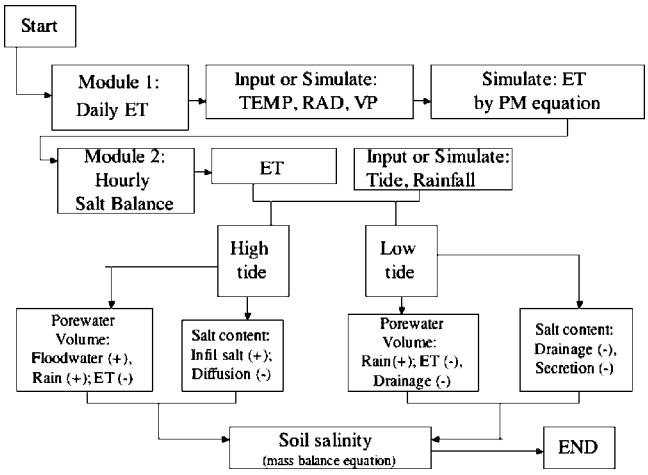

Fig. 1 – Flow diagram of the salt marsh salinity simulation model used in this study, modified from Morris (1995).

We added modifications to Morris' model primarily in four aspects. First, we used the Penman–Monteith equation (Allen et al., 1998; Hughes et al., 2001; Wang et al., 2003) to calculate daily ET given local climatic information (radiation, vapor pressure, temperature) instead of using a sine curve as in Morris' original model. The Penman–Monteith function has been shown to provide good estimates of ET in wetland ecosystems including salt marshes (e.g., Hughes et al., 2001; Jacobs et al., 2002). The details of the Penman–Monteith equation and ET estimation are given in Appendix A. Second, we considered the effect of soil temperature on saturated hydraulic conductivity (K_{sat}) in our modified simulation model. Morris (1995) used a constant hydraulic conductivity in the model. However, K_{sat} is found to increase with soil temperature because of the decrease in soil water viscosity (Hopmans and Dane, 1985). The details of this modification are described in Appendix B. Third, since not all of the rainfall enters the soil pedon, we calculated the infiltration rate of precipitation based on comparing rainfall intensity and soil infiltration capacity. Here infiltration capacity is determined by the saturated hydraulic conductivity, K_{sat}. Lastly, we set the soil moisture level for closure of drainage (i.e., gravitational flow = 0). In Morris' model, the minimum soil moisture level for closing drainage is the field capacity (Eqs. (9a–c) in Morris (1995)). We found that for marsh peat soils the field capacity is approximately 0.65 $m^3\,m^{-3}$ (volume at field capacity divided by total pedon volume, which would be 0.856 if divided by saturated vol-

ume), while for marsh sands the field capacity is close to 0.4 $m^3 m^{-3}$.

2.2. Data

Data from a salt marsh in the St. Marks National Wildlife Refuge (SMNWR) of northwestern Florida, USA (N30°05′, W84°10′) were used for model calibration and verification. This salt marsh is ideal for this modeling study because the incoming tide has relatively small variation in salinity and field data have been collected extensively during the last 20 years (e.g., Hsieh and Yang, 1992; Hsieh, 1996, 2004).

Data on soil properties such as hydraulic conductivity, bulk density, texture, field capacity, organic matter, and soil salinity were derived from laboratory analysis of field soil samples (0–30 cm depth, collected with a 5.1 cm diameter core sampler) from previous studies and this research. The methodology for field sample and laboratory analysis for soil moisture and soil salinity was given in Hsieh (2004). We also collected independent soil samples for each marsh zone for validation of our model (low marsh, middle marsh, border of middle marsh and salt barren, and center of salt barren); the mean values of two samples were used for each zone.

Climate data (daily air temperature, radiation, vapor pressure, and hourly rainfall) were acquired from the NOAA National Climatic Data Center (NCDC) and the Northwest Florida Water Management District (NWFWMD). Because no real-time monitoring tide station exists at this site, we used the predicted hourly tide data for our simulations taken from the NOAA Center for Operational Oceanographic Products and Services (CO-OPS) (http://www.co-ops.nos.noaa.gov). In a semi-diurnal tidal marsh, such as SMNWR, higher high water is the higher of the two high tides (Stumpf and Haines, 1998). The mean high water (MHW) level of semi-diurnal tide in SMNWR is 0.98 m, which is different from mean higher high water (MHHW = 1.04 m) because of the unequal amplitude of two highs in a day (Fig. 2). Average tide salinity of the area was 20 parts per thousand (ppt), with relatively small variability over time (Hsieh, 2004). We used the climate and tide data of the area during the period of 1999–2004 for the simulations. The parameters in the simulations are summarized in Table 1.

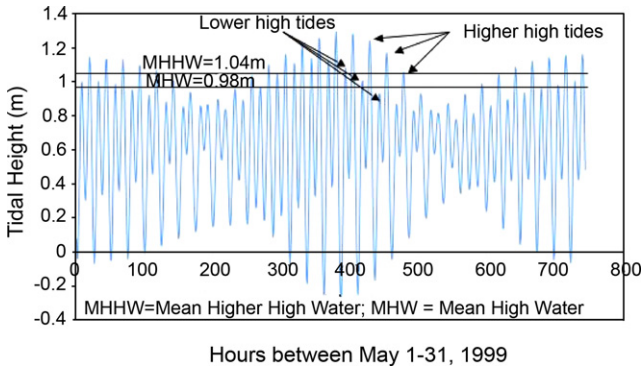

Fig. 2 – Illustration of a typical tidal regime for St. Marks National Wildlife Refuge indicating the difference between mean higher high water (MHHW) and mean high water (MHW).

2.3. Simulations and sensitivity analyses

We conducted simulations to examine the effects of tide, climate, soil properties, and vegetative factors on soil salinity distribution along the marsh topographic gradient. The simulation step interval was hourly. The outputs such as soil salinity along the elevational gradient and over time were reported in daily values. We calculated the average, maximum, and standard deviation of soil salinity along the marsh elevation gradient (from 0 to 1.5 m above the mean lower low water, or MLLW). The model was calibrated and validated by comparing simulated salinity with observed data.

2.3.1. Tide effects

For tide irregularity (defined here as the standard deviation of MHHW) on soil salinity, we first selected five stations along the Atlantic Coast and five along the Gulf of Mexico. We obtained tide data for these 10 stations from NOAA CO-OPS. All heights are referenced to MLLW. We computed MHW, MHHW, and its standard deviation (S.D.) for the sites. We found that the range of S.D. in MHHW for these stations was 0.1–0.44 m, which is 0.66–3.18 times the S.D. of SMNWR tide data. Thus, we generated simulated tide data with different values of S.D. (0.5–3.5

Table 1 – Parameters used in modeling the 30 cm pedon pore water salinity

Parameters	Meaning	This study	Morris (1995)
n	Porosity (ratio)	0.76	0.434–0.677
k_{sat}	Saturated hydraulic conductivity (cm h^{-1})	0.22	0.21–1.45
K_d	Salt diffusion coefficient ($cm^2 h^{-1}$)	0.0725	0.0725
Fc	Field capacity (ratio)	0.856	0.934–0.966
Wp[a]	Wilting point (ratio)	0.15	NA
k_2	Ion secretion factor (ratio)	0.03	0.03
k_3	Quotient of transpiration/ET (ratio)	0.5	0.5
r_a[b]	Aerodynamic resistance (s m^{-1})	2.0	NA
r_s[c]	Bulk surface resistance (s m^{-1})	5.0	NA

Porosity, hydraulic conductivity, and field capacity were derived from field samples.

[a] Coultas (1997).

[b] Hughes et al. (2001).

[c] Souch et al. (1998).

times S.D. at SMNWR) to examine the impact of tidal irregularity on soil salinity.

Besides the irregularity of tides in this area, we also conducted tests of the effects of tidal amplitudes on soil salinity distribution along the elevation gradient (0–3.5 m). Based on the analysis of tide data for these selected stations along the Atlantic and Gulf coasts, we found that MHHW ranged approximately ~0.5–6.0 m (mostly 0.5–2.5 m) along the Atlantic coastal regions, and ~0.3–2.0 m (mostly 0.5–1.0 m) for coastal areas along Gulf of Mexico (e.g., Stumpf and Haines, 1998). We adjusted the amplitude of MHHW using the SMNWR data in the range of 0.52–3.12 m, or 0.5–3 times the original MHHW at St. Marks for this analysis.

2.3.2. *Climate factors*

To evaluate the effects of air temperature on soil salinity, we simulated temperature as a sinusoidal function based on January minimum and July maximum temperatures of the eastern US regions in the form of:

$$T_{air}(\text{day}) = H + A\sin\left(\frac{2\pi\,\text{day}}{365} - 90\right) \quad (1)$$

where H is the shift of zero in y-axis and equals to January minimum temperature plus A, and A is amplitude of the sinusoidal function that equals to the half of the difference between July maximum temperature and January minimum temperature. We used the database of Atlantic and Gulf coasts from NOAA NCDC and selected six regions to represent the temperature gradient of the Eastern US, resulting in a range of January minimum temperature (−10.83 to 18.44 °C), July maximum temperature (26–33.5 °C), and mean annual temperature (7.6–25.2 °C) from Portland, Maine to Key West, Florida.

Along the Atlantic coast, the estimated mean ET ranged from ~1.04 to 1.74 mm day^{-1} in Maine to ~>2.44 mm day^{-1} in Florida and most of the Gulf coast (U.S. Geological Survey, 1990). The range corresponds to ~0.5–1.2 times ET in SMNWR (~2.41 mm day^{-1}) to evaluate the effects of ET on soil salinity.

The frequency or probability of rainfall occurrence was simulated using a two-state, first-order Markov Chain model, a stochastic and data-driven model in which the parameters defining each state and the estimated hourly sequence of states were derived from a historical record of SMNWR hourly rainfall occurrence. By a preliminary analysis of SMNWR hourly rainfall intensity, we found that there is an exponential distribution of the rainfall intensity in these data; therefore, we used an exponential distribution to derive the rainfall intensity for the rainy days. We wrote a FORTRAN program to simulate rainfall with different values for frequency, intensity, and combination of frequency and intensity, resulting in a total of 11 categories of rainfall patterns for the analyses.

2.3.3. *Soil properties*

For saturated hydraulic conductivity, K_{sat}, a range from 0.2 to 11.8 cm h^{-1} for salt marsh soils was used for the analysis (e.g., Coultas, 1997). The analysis of data from field water loggers (HOBO U20 water level logger, 3 min interval, weekly, from February to June 2004) deployed from low marsh, middle marsh, and salt barren to high marsh also showed a range of 0.18–12.89 cm h^{-1}, indicating a possible large variation in hydraulic conductivity among different types of salt marsh soils. Low to middle marshes with peat soils tend to have a lower K_{sat} (0.18–1.75 cm h^{-1}) than a salt barren with sandy soils (4.48–12.89 cm h^{-1}). For diffusion coefficient, K_d, there is a range from 0.018 to 0.035 cm^2 h^{-1} for ions in anoxic marine sediments, and 0.011 cm^2 h^{-1} for chloride in a subarctic marsh (e.g., Price and Woo, 1990). Morris (1995) used 0.0725 cm^2 h^{-1} for tidal marshes. We used 0.01–0.08 cm^2 h^{-1} for this study.

2.3.4. *Vegetation factors*

For k_3 (the quotient of transpiration/evapotranspiration), we used a range from 0.0 to 0.5; if in sandy non-vegetated soils, $k_3 = 0.0$, and in high marsh, $k_3 = 0.5$. Seaward, the proportion of evaporation to total ET caused by water surface increases should increase and, therefore, K_3 decreases. The aerodynamic resistance, r_a, is the resistance from the vegetation upward, which depends on friction from air flowing over vegetative surfaces. The bulk surface resistance, r_s, is the resistance of vapor flow through stomata openings, total leaf area, and soil surface (Allen et al., 1998). The surface resistance is zero under potential evaporation conditions (e.g., salt barren/flats). The aerodynamic resistance, r_a, ranged approximately from 2 to 20 s m^{-1} (e.g., Hughes et al., 2001; Wang et al., 2003), and the bulk surface resistance to water vapor, r_s, ranged from 5 to 40 s m^{-1}, the probable variability in salt marsh surface resistance; $r_s = 5.0$ s m^{-1} produced the best estimates of ET for salt marshes (e.g., Hughes et al., 2001) in the sensitivity analyses.

3. Results and discussion

3.1. *Model validation*

Our simulations showed a good agreement ($r^2 = 0.84$, $n = 15$, $P < 0.001$) with field observations (Fig. 3). The model produces a good agreement with observations for low marsh and middle marsh than salt barrens not only on the average values but also on the variations, i.e., SD of salinity (Fig. 4a). The degree of the agreement between our simulations and observations may change as sampling size, location, and seasons

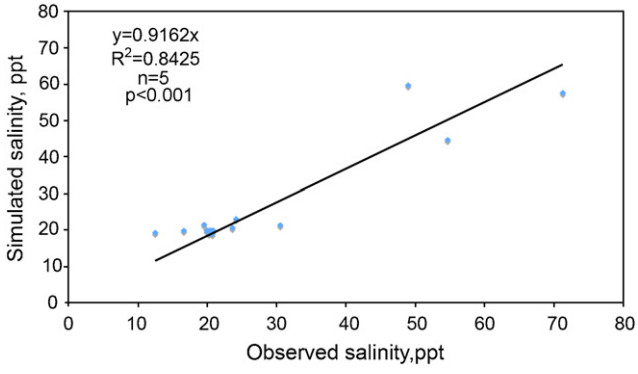

Fig. 3 – Comparison between simulated and observed soil salinity (0–30 cm) from low, middle, border of middle marsh and salt barren, and salt barren in St. Marks marshes during August–October 2004.

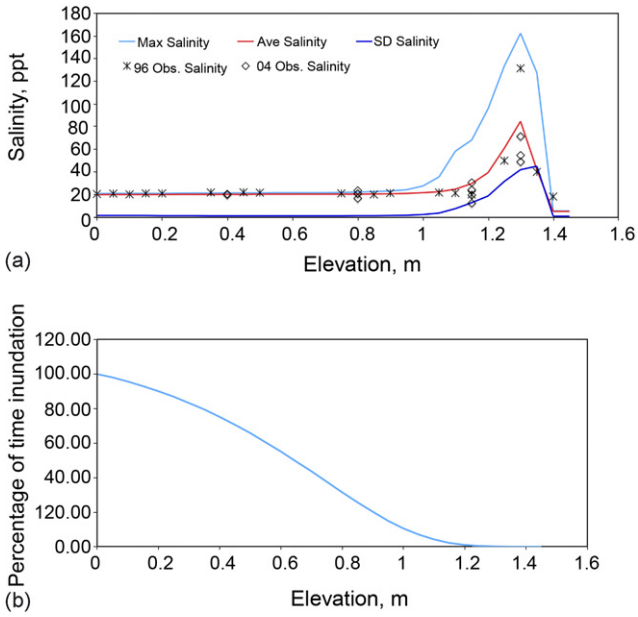

Fig. 4 – Soil salinity distribution of the salt marsh of the St. Marks National Wildlife Refuge (SMNWR) as predicted by the simulation modeling: (a) maximum, average, and standard deviation of soil salinity over time vs. field observations in 1996 (Hsieh, 2004) and 2004; (b) percentage of time of inundation vs. elevation above mean lower low water (MLLW).

in a year vary. Considering that the simulated salinity tended to be larger than 90 ppt for salt barrens for a year (Fig. 4a), the low observed salinity (71, 55, and 49 ppt) corresponded to the period (August–September 2004) after a series of hurricanes in 2004 in Florida, we conclude that our model is capable of describing the salinity gradient along the elevational gradient of a coastal marsh.

3.2. *Soil salinity gradient and tidal effects*

This simulation modeling study confirms the hypothesis that salt accumulation band at the vicinity of the high marsh zones in coastal marshes is caused by tidal action of saline water (Adam, 1990; Pennings and Bertness, 1999; Bertness and Pennings, 2000; Hsieh, 2004). At SMNWR, soil salinity of the low and middle marsh zones tends to reflect that of the incoming tide (i.e., here around 20 ppt). Soil salinity then increases to a maximum, $\sim 90 \pm 44$ ppt at 1.3 m elevation above MLLW, or approximately 25 cm vertically above MHHW. Salinity is then reduced to a lower level and quickly graded into the level of fresh-water at the border of upland forests (Fig. 4a) as observed by Hsieh (2004). This salt accumulation in a marsh is a result of the balance between salt inputs (tide) and outputs (drainage and diffusion). That is, infrequent tidal inundation at the vicinity of high marsh area allows a chance for ET to concentrate seawater and minimizes salt output due to drainage. For the case of SMNWR, salt accumulation becomes detectable when tidal inundation is less than 7% of the time (Fig. 4b). Salinity variation in this salt accumulation band is also much greater than that in the low and middle marsh zones in the simulation (Fig. 4a), which agrees with the observation (Hsieh, 2004).

3.2.1. *Soil salinity maximum*

The salinity distribution along a marsh elevational gradient predicted from our simulations (Fig. 4a) is consistent with the salinity distribution found by many previous field studies (e.g., Fig. 2 in Hsieh, 2004). On the other hand, Pennings and Bertness (1999) stated that there would be no such salinity accumulation band in the salt marshes of high latitude such as those in the New England (see also the review by Mahall and Park, 1976a). Our simulations, however, indicate that there still should be a salinity maximum band, although to a lesser extent, even at New English salt marshes. Bertness and Pennings (2000) proposed a climate-driven salt flat hypothesis and suggested that the presence of salt barrens/flats/pannes in southern but not northern marshes is driven by latitudinal variation in climate. Our results offer simulation evidence to this hypothesis. ET and temperature largely control the extent of salt accumulation in marshes. Higher ET and temperatures at lower latitudes are necessary to achieve the development of hypersaline conditions that eliminates vegetation and forms tidal salt barrens in the low latitude marshes (Hsieh, 2004).

As to what is the threshold salinity condition for a tidal salt barren to develop, no empirical studies have provided a definite answer yet. Adams (1963) reported that an average soil salinity of 70 ppt would prevent the establishment and survival of most salt marsh species. If the salinity threshold is 70 ppt for tidal salt barren formation, we would infer that the northern thermal boundary for the occurrence of a salt barren is likely at locations with mean annual temperature under 7 °C (Fig. 5a), given the conditions of tides, soil properties, and vegetation factors similar to SMNWR. Nevertheless, in reality, whether or not a salt barren can be formed in a marsh depends on the interactions between climate (mostly ET and temperature) and the salinity of the incoming tide.

The soil salinity gradient is not simply related to marsh elevation, but also to micro-topography, creek pattern, and geomorphology that affect the drainage of marsh soils (e.g., Davy, 2000). For example, other factors being equal, increasing hydraulic conductivity from 0.2 to 5 cm h^{-1} could reduce soil salinity maximum from 90 ppt to <70 ppt (Fig. 6a), consequently allowing the survival and growth of some highly salt-tolerant species. Therefore, it is not surprising to know that there are tidal salt barrens with soil salinity above 100 ppt along the Virginia coasts where mean annual temperature is approximately 15 °C (Santos and Zieman, 2005). The Virginia coast was thought to be near the latitudinal limit of tidal salt barren formation on the US Atlantic coast (Santos and Zieman, 2005). If this hypothesis is true, or if the minimum mean annual temperature for the occurrence of salt barrens/flats is ~15 °C, then it is most likely that soil hydraulic properties and the salinity of incoming tide would control the soil salinity maximum at locations with mean annual temperature in the range of 7–15 °C. In fact, Santos and Zieman (2005) found that soil/sediment hydraulic properties and microclimate are the main variables that account for more than 58% of the variation in soil salinity.

The potential for the occurrence of salt barrens/flats would be reduced dramatically if salt marshes receive a large amount

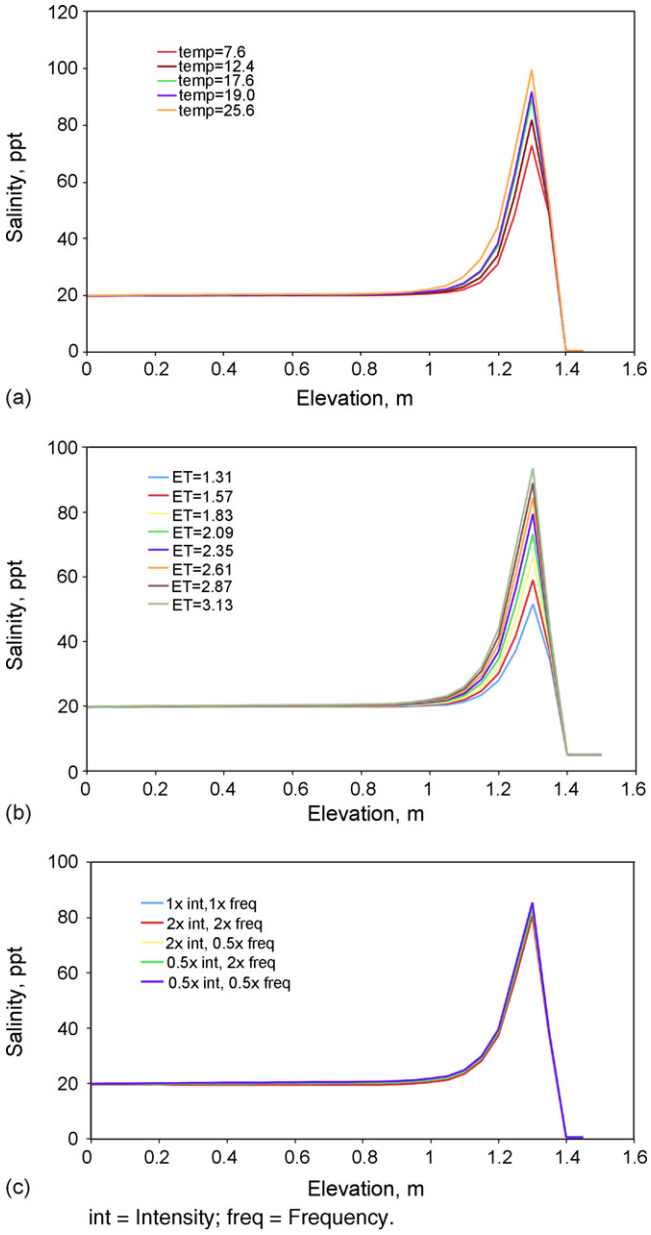

Fig. 5 – Effects on soil salinity distribution along salt marsh elevational gradient above MLLW of: (a) air temperature (°C); (b) ET (mm day^{-1}); (c) frequency and intensity of rainfall.

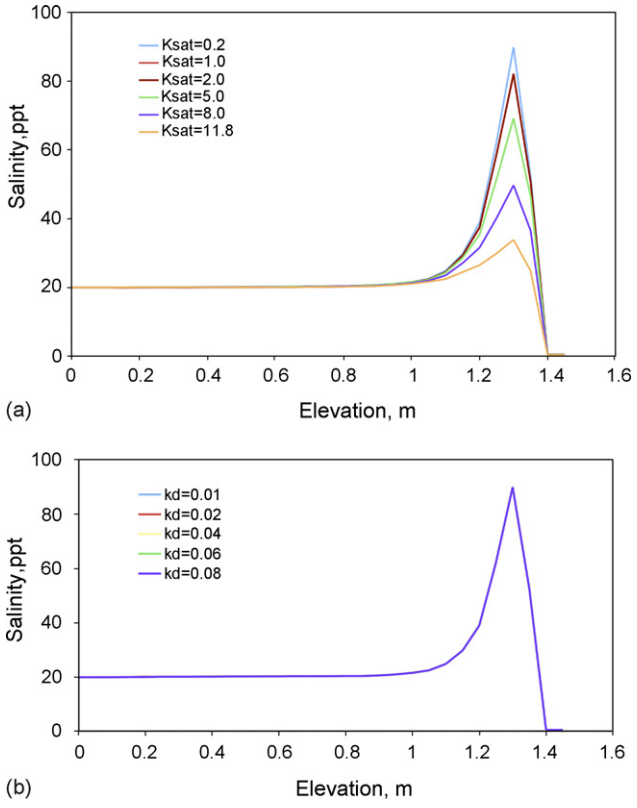

Fig. 6 – Effects on soil salinity distribution along salt marsh elevational gradient above MLLW of soil physical properties: (a) hydraulic conductivity (K_{sat}, cm h^{-1}); (b) diffusion coefficient of salt (K_d, cm^2 h^{-1}).

of freshwater input from upland with less salt input. Therefore, salt barrens/flats tend to appear in tide-dominated salt marshes, not river-dominated salt marshes (Hsieh, 2004). One example is that salt barrens are found in the tide-dominated SMNWR but not in the nearby river-dominated Apalachicola Bay where large amounts of freshwater input from Apalachicola River and upland diluted the salinity (e.g., Huang et al., 2002).

3.2.2. *The salinity–elevation relationship and apparent shapes of salinity maximum in marshes*

Our simulations indicate that soil salinity in a marsh is related to the topography (elevation) of the marsh. Tidal irregularity (variation in the MHHW) is the primary control on the width of the salinity accumulation band in a marsh. The more irregular the MHHW, the wider the salinity accumulation band would be (Fig. 7a and c). For example, the width of salinity accumulation band increased from ~0.3 m to ~1.5 m (elevational difference) when the irregularity of MHHW increases from 1.04 ± 0.09 m to 1.04 ± 0.436 m above MLLW. Pennings and Callaway (1992) also found that soil salinity increases with elevation from MHHW to the upper edge of salt flats. This simple "salinity–elevation" relationship is manifested in a much more complicated two-dimensional manner because of the tidal channel network. For example, the salinity maximum band, such as tidal salt barren, can be found as irregular belts and circles around tree islands and topographic maximum (Hsieh, 2004).

3.2.3. *Location of soil salinity maximum*

Similar to the effects of tidal irregularity, tidal amplitude and MHHW level did not affect the magnitude of salinity in a marsh. Instead, it influences the location of the maximum salinity along the topographic gradient (Fig. 7b). It is well known that soil salinity reaches a maximum at a location above mean high water (MHW) or mean higher high water (MHHW) (Stumpf and Haines, 1998; Adam, 1990). However, there are no empirical studies that have quantified the relationship between the location of the salinity maximum and MHW or MHHW. Adam (1990) indicated that mean high water spring (MHWS) or MHHW level controls the location of the

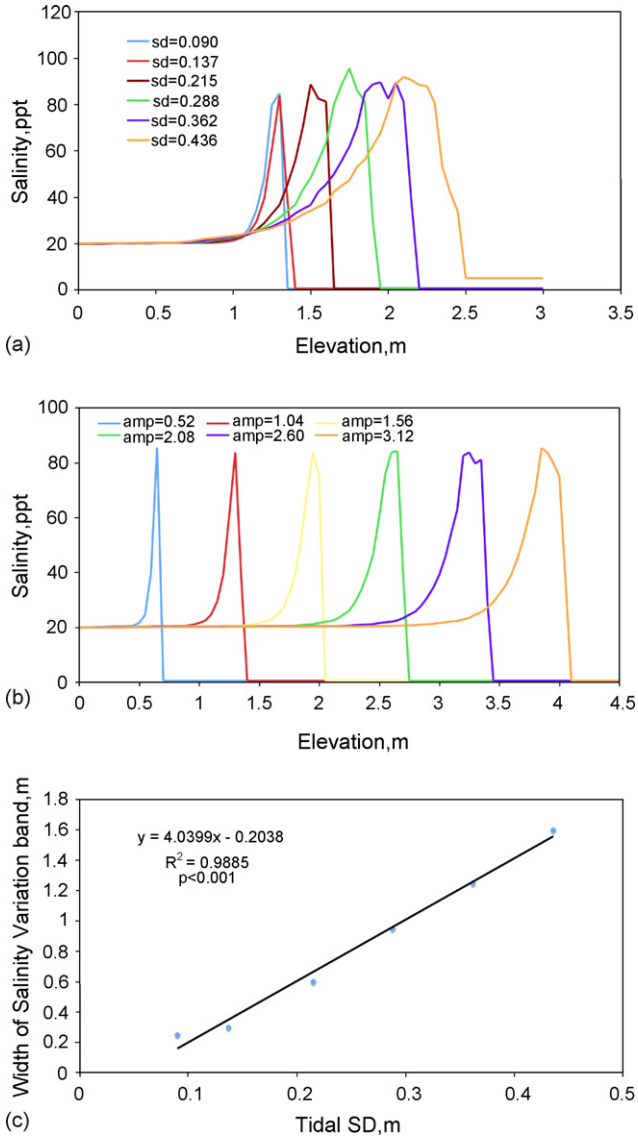

Fig. 7 – Effects on soil salinity distribution along salt marsh elevational gradient above MLLW of: (a) tidal irregularity (S.D., m); (b) tidal amplitude (m). The relationship between tidal irregularity (S.D.) and width of salinity variation band is shown in (c).

salinity maximum. Our simulations support this observation. For a site with semi-diurnal tides having very similar two high tides or a site with diurnal tides, then MHW is equal to MHHW. At these situations, one can say that MHW determines the location of soil salinity maximum. But in other situations where MHHW does not equal MHW, as the case in SMNWR (Fig. 2), it is MHHW (corresponding to mean spring tide elevation) not MHW that determines the location of the soil salinity maximum.

3.3. *Factors affecting soil salinity maximum*

We summarized the sensitivity of soil salinity maximum, location, and width of salt accumulation band to different environmental factors listed in Table 2. The soil salinity maximum tends to be highly sensitive to ET, temperature, hydraulic conductivity, and bulk surface resistance, whereas the width of the soil salinity accumulation band tends to be highly sensitive to tidal irregularity. Pearson correlation analyses between the soil salinity maximum and the parameters of the model indicated that ET, temperature, hydraulic conductivity, and bulk surface resistance to water vapor are significant factors that control salt accumulation in a coastal marsh (Table 3). ET and the mean annual temperature have positive correlations with salinity maximum, whereas hydraulic conductivity and bulk surface resistance to water vapor have negative correlations with salinity maximum. This result implies that variations in thermal dynamics, soil physical properties that determine hydrological processes such as soil texture, and characteristics of vegetation and topography mainly control the soil salinity distribution in salt marshes of the Atlantic and Gulf coastal regions.

3.3.1. *Climatic factors*

Temperature profoundly affects salt accumulation in a coastal marsh. Our model results showed that as the average temperature of a region increases from 7.6 to 25.6 °C, salinity maximum increased from 72 to 100 ppt (Fig. 5a) when incoming tidal salinity was at 20 ppt. According to the simulations, the temperature effect on the salinity maximum of a marsh can be expressed in the following equation (Fig. 8a):

$$y = 0.0771x + 3.1058; \quad r^2 = 0.9879; \quad P < 0.001 \tag{2}$$

where y is the soil salinity concentration ratio (SCR), i.e., the ratio of the average salinity at the salinity maximum to that

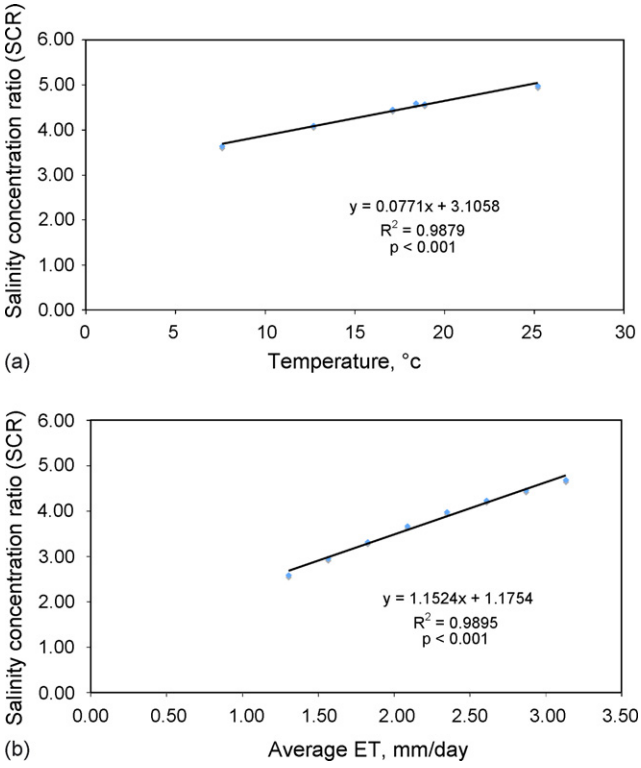

Fig. 8 – Relationships between soil salinity maximum (per unit of incoming tidal salinity) and (a) temperature (°C); (b) evapotranspiration (ET, mm day^{-1}).

Table 2 – Summary of the sensitivity analyses of the effects of climatic, tidal, and soil properties on soil salinity maximum and variation band width

Parameters	Range	Sensitivity on maximum	Sensitivity on band width
Mean annual temperature (°C)	7.6–25.2	High	Medium
ET (mm day^{-1})	1.31–3.13	High	Medium
Rainfall intensity (mm year^{-1})	767.53–3097.45	Low	Low
Rainfall frequency	0.5x–2.0x	Low	Low
Tidal irregularity (m)	0.09–0.436	Low	High
Tidal amplitude (m)	0.52–3.12	Low (but high on location)	Low
Hydraulic conductivity (k_{sat}, cm h^{-1})	0.2–11.8	High	Low
Salt diffusion coefficient (k_d, cm^2 h^{-1})	0.01–0.08	Low	Low
Quotient of transpiration/ET (k_3)	0.0–0.5	Low	Low
Aerodynamic resistance (r_a, s m^{-1})	2.0–20.0	Medium	Low
Bulk surface resistance (r_s, s m^{-1})	5.0–40.0	High	Medium

of the incoming tide, x is temperature in °C. Temperature has little effect on the salinity of the low and middle marsh zones where tidal inundation is greater than 7% of the time.

Since ET is closely related to temperature, it also greatly affects the salt salinity maximum in a marsh. Soil salinity maximum at the SMNWR increased from 51 to 94 ppt as ET increased from 1.3 to 3.1 mm day^{-1} given the incoming tidal salinity of 20 ppt (Fig. 5b). When the ET–salinity relationship was expressed in SCR (Fig. 8b), we obtained:

$$y = 1.1524x + 1.1754; \quad r^2 = 0.9895; P < 0.001 \qquad (3)$$

where y is SCR, x is average ET in mm day^{-1}.

Compared with temperature and ET, rainfall does not have as great an effect on soil salinity accumulation in a marsh. An increase in rainfall intensity and frequency tends to reduce salinity (Fig. 5c). For example, doubling both rainfall intensity and frequency (from ~750 to 3000 mm year^{-1}) just slightly reduced the salinity maximum from 85.2 to 80.6 ppt. Considering that annual rainfall along the Atlantic coast from Maine to Florida varies between ~1080 and 1380 mm, it can be concluded that rainfall has a minor impact on salt accumulation in a coastal marsh. It is not surprising that rainfall does not affect soil salinity at locations below MHHW, as rainfall cannot compete with tides in influencing the porewater salinity. Soil salinity below MHHW is controlled by the salinity of tidal water (e.g., De Leeuw et al., 1991). There is a difference in rainfall effects on soil salinity for sites above MHHW. Our simulations showed trivial influence of rainfall impact. However, it should be noted that the minor impact of rainfall on soil salinity distribution does not necessarily mean that rainfall would not affect the variation in short-term (e.g., seasonal, daily, or hourly) salinity for locations well above MHHW. In fact, rainfall deficit is important to the seasonal changes in soil salinity. Previous studies have found that rainfall deficit (rainfall-evapotranspiration) controls soil salinity at high marshes by regulating the seasonal and interannual patterns of soil salinity (e.g., De Leeuw et al., 1991). Heavier summer rainfall could reduce salt built-up at more southern sites. Rainfall can provide a major source of freshwater to the upland areas including river systems that drain into coastal salt marshes, resulting in decreased soil salinity through dilution.

Table 3 – Pearson correlation statistics between biophysical factors and soil salinity at the location where salinity maximum occurs along the elevational gradient

Factor	n	Pearson correlation	P
ET	8	0.995	0.001
Temperature	6	0.994	0.001
k_{sat}	6	−0.994	0.001
r_a	4	0.881	0.119
r_s	8	−0.939	0.002

Significance level was set at 0.01. k, saturated hydraulic conductivity; r_a, aerodynamic resistance; r_s, bulk surface resistance.

3.3.2. *Soil properties*

Other factors being equal, in general higher saturated hydraulic conductivity (K_{sat}) tends to result in lower soil salinity at the salt accumulation band of a marsh (Fig. 6a). From observations at SMNWR, we found that gravitational soil water flow stopped at 85% moisture level on a dry soil weight basis. This property of strongly retaining water in salt marsh soils was included in the model simulation and found very important to the accuracy of this simulation modeling.

We found that hydraulic conductivity is as important a factor as ET and temperature in determining soil salinity accumulation in a marsh. In tidal salt marshes, it was found that water table response to tidal forcing is determined largely by soil hydraulic conductivity (e.g., Hughes et al., 1998; Silvestri et al., 2005). Higher hydraulic conductivity results in lower soil salinity because water rapidly moves out of the soil, flushing the soil and minimizing salt build-up (Bertness and Pennings, 2000). Our result is consistent with Morris (1995) on this aspect. However, the effect of hydraulic conductivity on salinity in our sensitivity analysis is much higher than that of Morris (1995), which characterized the influence as slight. This discrepancy is presumably caused by the difference in conductivity range used and the location where effects were examined. Our conductivity range (0.2–11.8 cm h^{-1}) is much larger than Morris' (0.21–1.45 cm h^{-1}), which is at the lower end of our range.

Our analysis showed that at the lower end of the conductivity range, the effect on salinity was minor. Moreover, the elevation (0.58 m) of the study site in Morris (1995) was near mean high water (MHW) rather than at maximum salinity, which would be near 0.83 m elevation at this site. If the analysis were done at an elevation of 0.83 m and with a larger range of hydraulic conductivity, the influence of conductivity on salinity would be substantial even at Morris' site, i.e.,

North Inlet, South Carolina. For example, at the SMNWR, if we use the MHHW of 1.05 m, the salinity would change less than 4% over the conductivity range of 0.2–11.8 cm h^{-1}; but if we use the salinity maximum elevation of 1.3 m, the corresponding salinity change would be more than 60%. Therefore, any biotic and abiotic factor that causes a dramatic change in soil hydraulic conductivity of marsh soils would have the potential to impact the soil salinity accumulation significantly.

Very low effect of diffusion coefficient on soil salinity was seen in the sensitivity analyses (Fig. 6b). This is because diffusion of salt is a small-scale process that occurs close to the marsh plants' roots and depends on the magnitude of the gradient of salt concentration resulting from salt accumulation (e.g., Hollins et al., 2000).

3.3.3. *Vegetative factors*

Quotient of transpiration/ET, K_3: there are minor effects of K_3 on soil salinity in a marsh, although higher K_3 tends to lower soil salinity (Fig. 9a). Higher quotient of transpiration/ET means a higher proportion of plant transpiration, which tends to lead to a higher removal of salt by diffusion. This is in contrast to salt left in the soil by evaporation without loss if ET involves only evaporation.

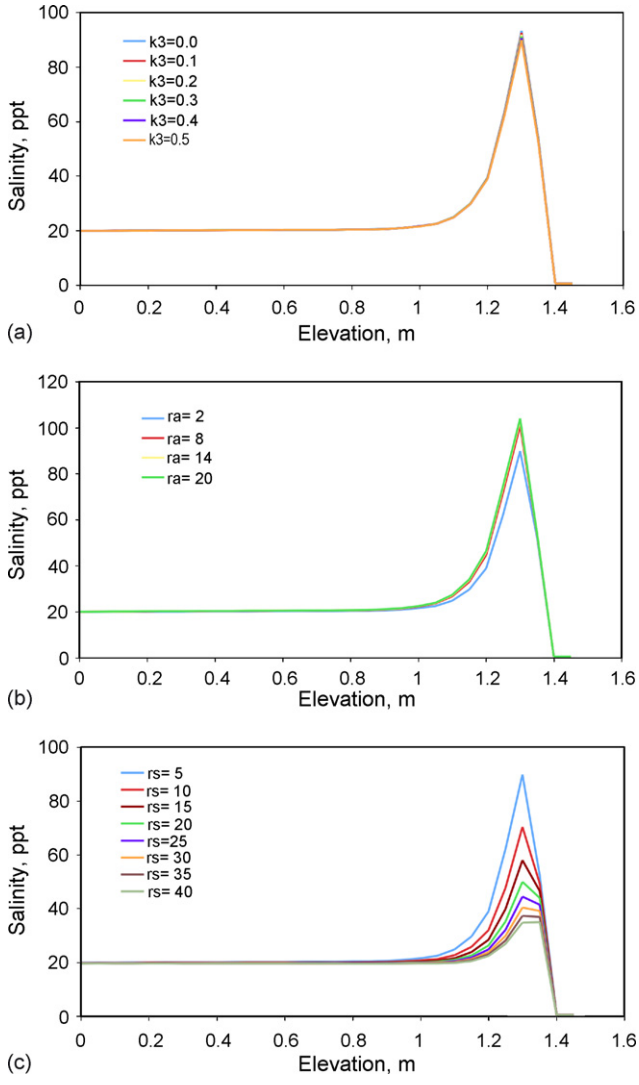

Fig. 9 – Effects on soil salinity distribution along salt marsh elevational gradient above MLLW of vegetative factors: (a) ratio of transpiration to ET (K_3); (b) aerodynamic resistance (r_a, s m^{-1}); (c) bulk surface resistance to water vapor (r_s, s m^{-1}).

Canopy aerodynamic resistance, r_a, tends not to affect soil salinity significantly, although higher aerodynamic resistance would increase salinity (Fig. 9b). Past studies using the Penman–Monteith equation have indicated that aerodynamic resistance is an important parameter in estimating transpiration (e.g., Wang et al., 2003). The aerodynamic resistance is dependent largely upon plant height, roughness, and wind speed (Allen et al., 1998; Hughes et al., 2001). On the other hand, the bulk surface resistance, r_s, does significantly affect soil salinity (Fig. 9c). The higher the surface resistance, the lower the soil salinity. This is primarily caused by the decrease in ET; thus the reduced salt accumulation results from increasing surface resistance. For example, Hughes et al. (2001) found that increasing surface resistance from 0 to 40 s m^{-1} resulted in the decrease in ET by up to 2 mm day^{-1}. The surface resistance is an important ecophysiological parameter, which tends to vary with plant species, plant cover (e.g., leaf area index, LAI), water availability, and climate (e.g., radiation intensity, temperature, and vapor pressure deficit) (Allen et al., 1998; Hughes et al., 2001). Because of the substantial variation in climate, a greater difference in bulk surface resistance is expected for salt marshes along the latitudinal gradient, resulting in the significant variation in the salt accumulation band in a marsh. Overall, both the aerodynamic resistance and bulk surface resistance influence ET rate in salt marshes (e.g., Hughes et al., 2001; Jacobs et al., 2002). Therefore, vegetation affects soil salinity primarily through the influence of these two resistance factors on ET.

Acknowledgements

This research was supported by funding from the US Environmental Protection Agency (EPA STAR Grant # RD-83088001) to the Environmental Sciences Institute (ESI), Florida A&M University (FAMU), and funding from the National Oceanic and Atmospheric Administration (NOAA) to the Environmental Cooperative Science Center (ECSC) at FAMU (NOAA Cooperative Agreement # NA17AE1624). We thank Glynnis Bugna Djanan Nemours, Nick Wooten, Elijah Johnson, and Katherine Milla for their assistance and comments during the course of this work. We also acknowledge the anonymous reviewers for their insightful comments and suggestions to improve the manuscript.

Appendix A. ET estimation using Penman–Monteith equation

The Penman–Monteith equation is

$$\lambda ET = \frac{\Delta(R_n - G) + (P_a C_p VPD/r_a)}{\Delta + \gamma(1 + (r_s/r_a))} \quad (A.1)$$

where λ is latent heat of vaporization, 2.45 MJ kg^{-1}, ET is daily evapotranspiration rate in mm day^{-1}, Δ is the slope of the saturation vapor pressure curve at air temperature in (kPa °C^{-1}); and

$$\Delta = \frac{2504 \exp[17.27T_{air}/T_{air} + 237.3]}{(T_{air} + 237.3)^2} \quad (A.2)$$

where T_{air} is air temperature, °C; R_n is net radiation; MJ m^{-2} day^{-1}, and (Hughes et al., 2001);

$$R_n = 0.63R_s - 2.01 \quad (A.3)$$

where R_s is incoming short-wave solar radiation, and (Allen et al., 1998);

$$R_s = \left[a_s + b_s \frac{n}{N}\right] R_a \quad (A.4)$$

where $a_s = 0.25$, $b_s = 0.5$; n/N is the ratio of actual (n) to maximum possible (N) sunshine hours, first assume $n/N = 1$ then $R_s = 0.75R_a$, where R_a is extraterrestrial radiation; G the soil heat flux, MJ m^{-2} day^{-1}, and G the small compared to R_n and may often be ignored = 0 (Allen et al., 1998); P_a is the mean air density at constant pressure (kg m^{-3}), and (Allen et al., 1998);

$$P_a = \frac{P}{T_{kv}R} \quad (A.5)$$

where P is atmosphere pressure (kPa), = 101.3 kPa for costal areas; T_{kv} the virtual temperature that is used to find the density of a parcel of air at a constant pressure level (=1.01 × (T_{air} + 273)); R the specific gas constant (= 0.287 kJ kg^{-1} K^{-1}); C_p the specific heat of air, 1.013 × 10E−3, MJ kg^{-1} °C^{-1}; VPD is the vapor pressure deficit, kPa; VPD = SVP − WVP, and

$$SVP = 0.6108 \exp\left[\frac{17.27T_{air}}{T_{air} + 237.3}\right] \quad (A.6)$$

in kPa; r_a is aerodynamic resistance (s m^{-1}), which is a function of wind speed at 2 m, r_a ranges from 2 to 20 s m^{-1} in wetland ecosystems, using 2 s m^{-1} in our simulation (e.g., Hunt et al., 1997); r_s the bulk surface resistance to water vapor (=5–40 s m^{-1}, often =5.0 s m^{-1}; e.g., Hughes et al., 2001); γ is psychometric constant (=0.0673 kPa °C^{-1}).

Then, daily ET was assigned to hourly ET from 600 to 1800 using the same protocol as in Morris (1995):

$$ET(t) = \frac{-(t^2 - 24t + 144)ET}{288} + 0.125ET \quad \text{for } 6 < t \leq 18 \quad (A.7a)$$

$$ET(t) = 0 \quad \text{for } 6 \geq t > 18 \quad (A.7b)$$

We closed hourly ET when rainfall occurs.

Appendix B. Soil temperature effect

Hydraulic conductivity is a function of soil temperature that affects soil water viscosity (Hopmans and Dane, 1985):

$$K_T = \left[\frac{\eta_{ref}}{\eta_T}\right] K_{ref} \quad (B.1)$$

where η_{ref} and η_T are the viscosity of water at the reference temperature and the soil temperature of interest, respectively; and K_{ref} is the hydraulic conductivity at the reference temperature, here assigned as 0.2 cm h^{-1} from experiments based on room temperature (20 °C) as the reference temperature. In this equation, it is assumed that the changes in water density with temperature are negligible. The ratio, η_{ref}/η_T, can be described by a linear function:

$$\frac{\eta_{ref}}{\eta_T} = 0.032T + 0.2928 \quad (r^2 = 0.9963) \quad (B.2)$$

Soil temperature is simulated as a sinusoidal function of air temperature using the equation developed by Hillel (1982):

$$T(z, t) = T_a + A_0 e^{-z/d} \sin\left[\frac{2\pi(t - t_0)}{365} - \frac{z}{d} - \frac{\pi}{2}\right] \quad (B.3)$$

where T_a is average soil surface temperature, °C, assumed equal to average air temperature; A_0 the annual amplitude of the surface soil temperature in °C, and is one-half of the difference between annual averaged maximum air temperature and minimum air temperature (Kasuda and Archenbach, 1965); z the soil depth, 30 cm; t_0 the time lag, in days, or day of the year of the minimum surface temperature and assumed in the middle of January; d is the damping depth, m, and

$$d = \sqrt{\frac{2D_h}{w}} \quad (B.4)$$

where D_h is thermal diffusivity, and = 5.56 × 10E−7 m^2 S^{-1} (Elias et al., 2004); and $w = 2\pi 365^{-1}$ day^{-1}.

REFERENCES

Adams, D.A., 1963. Factors influencing vascular plant zonation in North Carolina salt marshes. Ecology 44, 445–456.

Adam, P., 1990. Saltmarsh Ecology. Cambridge University Press, Cambridge.

Allen, R.G., Pereira, L.S., Raes, D., Smith, M., 1998. Crop Evapotranspiration: Guidelines for Computing Crop Water Requirements. Food and Agriculture Organization of the United Nations, Rome, Italy.

Bertness, M.D., Pennings, S.C., 2000. Spatial variation in process and pattern in salt marsh plant communities in eastern North America. In: Weinstein, M.P., Kreeger, D.A. (Eds.), Concepts and Controversies in Tidal Marsh Ecology. Kluwer Academic Publishers, Norwell, MA, USA.

Callaway, R.M., Jones, S., Ferren Jr., W.R., Parikh, A., 1990. Ecology of a Mediterranean-climate estuarine wetland at Carpinteria, California: plant distribution and soil salinity in the upper marsh. Can. J. Bot. 69, 1139–1146.

Coultas, C.L., 1997. Soils. In: Coultas, C.L., Hsieh, Yuch-Ping (Eds.), Ecology and Management of Tidal Marshes. A Model from the Gulf of Mexico. St. Lucie Press.

Davy, A.J., 2000. Development and structure of salt marshes: community patterns in time and space. In: Weinstein, M.P., Kreeger, D.A. (Eds.), Concepts and Controversies in Tidal Marsh Ecology. Kluwer Academic Publishers, Norwell, MA, USA.

De Leeuw, J., Van den Dool, A., De Munk, W., Nieuwehuize, J., Beeftink, W.G., 1991. Factors influencing the soil salinity

regime along an intertidal gradient. Estuar. Coast. Shel. 32, 87–97.
Elias, E.A., Cichota, R., Torriani, H.H., VanLier, Q.J., 2004. Analytical soil-temperature model: correction for temporal variation of daily amplitude. Soil Sci. Soc. Am. J. 68, 784–788.
Hillel, D., 1982. Introduction to Soil Physics. Academic Press, San Diego, CA, USA.
Hollins, S.E., Ridd, P.V., Read, W.W., 2000. Measurement of the diffusion coefficient for salt in salt flat and mangrove soils. Wetland Ecol. Manage. 8, 257–262.
Hopmans, J.W., Dane, J.H., 1985. Effect of temperature-dependent hydraulic properties on soil water movement. Soil Sci. Soc. Am. J. 49, 51–58.
Hsieh, Y.P., 1996. Assessing aboveground net primary production of vascular plants in marshes. Estuaries 19, 82–85.
Hsieh, Y.P., 2004. Dynamics of tidal salt barren formation and the record of present-day sea level change. In: Fagherazzi, S., Marani, M., Blum, L.K. (Eds.), The Ecogeomorphology of Tidal Marshes. Coastal and Estuarine Studies, vol. 59. American Geophysical Union, Washington, DC, USA.
Hsieh, Y.P., Yang, C.H., 1992. A method for quantifying living roots of *Spartina* (Cordgrass) and *Juncus* (Needlerush). Estuaries 15, 414–419.
Huang, W., Jones, W.K., Wu, T.S., 2002. Modeling wind effects on subtidal salinity in Apalachicola Bay, Florida. Estuar. Coast. Shel. 55, 33–46.
Hughes, C.E., Binning, P., Willgoose, G.R., 1998. Characterization of the hydrology of an estuarine wetland. J. Hydrol. 211, 34–49.
Hughes, C.E., Kalma, J.D., Binning, P., Willgoose, G.R., Vertzonis, M., 2001. Estimating evapotranspiration for a temperate salt marsh, Newcastle, Australia. Hydrol. Process. 15, 957–975.
Hunt, R.J., Krabbenhoft, D.P., Anderson, M.P.L., 1997. Assessing hydrogeochemical heterogeneity in natural and constructed wetlands. Biogeochemistry 39, 271–293.
Jacobs, J.M., Mergelsberg, S.L., Lopera, A.F., Myers, D.A., 2002. Evapotranspiration from a wet prairie wetland under drought conditions: Paynes Prairie Preserve, Florida, USA. Wetlands 22, 374–385.
Kasuda, T., Archenbach, P.R., 1965. Earth temperature and thermal diffusivity at selected stations in the United States. ASHRAE Trans. 71 (Part 1).
Mahall, B.E., Park, R.B., 1976a. The ecotone between *Spartina foliosa* Trin. and *Salicornia virginica* L. in salt marshes of northern San Francisco Bay. I. Biomass and production. J. Ecol. 64, 421–433.
Mahall, B.E., Park, R.B., 1976b. The ecotone between *Spartina foliosa* Trin. and *Salicornia virginica* L. in salt marshes of northern San Francisco Bay. II. Soil water and salinity. J. Ecol. 64, 793–809.
Morris, J.T., 1995. The mass balance of salt and water in intertidal sediments: results from North Inlet, South Carolina. Estuaries 18, 556–567.
Pennings, S.C., Callaway, R.M., 1992. Salt marsh plant zonation: the relative importance of competition and physical factors. Ecology 73, 681–690.
Pennings, S.C., Bertness, M.D., 1999. Using latitudinal variation to examine effects of climate on coastal salt marsh pattern and process. Curr. Top. Wetl. Biogeochem. 3, 100–111.
Pennings, S.C., Grant, M., Bertness, M.D., 2005. Plant zonation in low-latitude salt marshes: disentangling the roles of flooding, salinity and competition. J. Ecol. 93, 159–167.
Price, J.S., Woo, M.H., 1990. Studies of a subarctic coastal marsh. III. Modeling the subsurface water fluxes and chloride distribution. J. Hydrol. 120, 1–13.
Santos, M.C.F.V., Zieman, J.C., 2005. The salt flats of the VCR-LTER: a synthesis. http://www.vcrlter.virginia.edu/gopher/Publications/VCRAdmin/1994ASC/Santos.html.
Silvestri, S., Marani, M., 2004. Salt-marsh vegetation and morphology: basic physiology, modeling and remote sensing observations. In: Fagherazzi, S., Marani, M., Blum, L.K. (Eds.), The Ecogeomorphology of Tidal Marshes. Coastal and Estuarine Studies, vol. 59. American Geophysical Union, Washington, DC, USA.
Silvestri, S., Defina, A., Marani, M., 2005. Tidal regime, salinity and salt marsh plant zonation. Estuar. Coast. Shel. 62, 119–130.
Souch, C., Grimmond, C.S.B., Wolfe, C.P., 1998. Evapotranspiration rates from wetlands with different disturbance histories: Indianan Dunes National Lakeshore. Wetlands 18, 216–229.
Stumpf, R.P., Haines, J.W., 1998. Variations in tidal level in the Gulf of Mexico and implications for tidal wetlands. Estuar. Coast. Shel. 46, 165–173.
U.S. Geological Survey, 1990. National water summary 1987-Hydrologic events and water supply and use: U.S. Geological Survey Water-Supply Paper 2350, 553 p.
Wang, H., Hall, C.A.S., Scatena, F.N., Fetcher, N., Wu, W., 2003. Modeling the spatial and temporal variability in climate and primary productivity across the Luquillo Mountains, Puerto Rico. Forest Ecol. Manage. 179, 69–94.